Published in "The Plant Cell 25(1): 202-214, 2013"
which should be cited to refer to this work.

Supplemental Data

TWISTED DWARF1 functionally interacts with auxin exporter ABCB1 on the root plasma membrane

Bangjun Wang[1, 2, 3, 10], Aurélien Bailly[1, 2, 7, 10], Marta Zwiewka[4], Sina Henrichs[2], Elisa Azzarello[5], Stefano Mancuso[5], Masayoshi Maeshima[7], Jiri Friml[4], Alexander Schulz[3], Markus Geisler[1, 2, 8, 9]

[1] University of Fribourg, Department of Biology - Plant Biology, Fribourg, Switzerland

[2] University of Zurich, Institute of Plant Biology, Zurich, Switzerland

[3] University of Copenhagen, Department of Plant and Environmental Sciences, Frederiksberg, Denmark

[4] University of Gent, Department of Plant Systems Biology, Gent, Belgium

[5] Department of Horticulture, University of Firenze, Sesto Fiorentino, Italy

[6] Plant Science Education Unit, Graduate School of Biological Sciences, Nara Institute of Science and Technology, Nara, Japan

[7] present address: University of Zurich, Institute for Plant Biology, Department of Microbiology

[8] to whom correspondence should be addressed: markus.geisler@unifr.ch

[9] The author responsible for distribution of materials integral to the findings presented in this article in accordance with the policy described in the Instructions for Authors (www.plantcell.org) is: Markus Geisler (markus.geisler@unifr.ch).

[10] These authors contributed equally to this work.

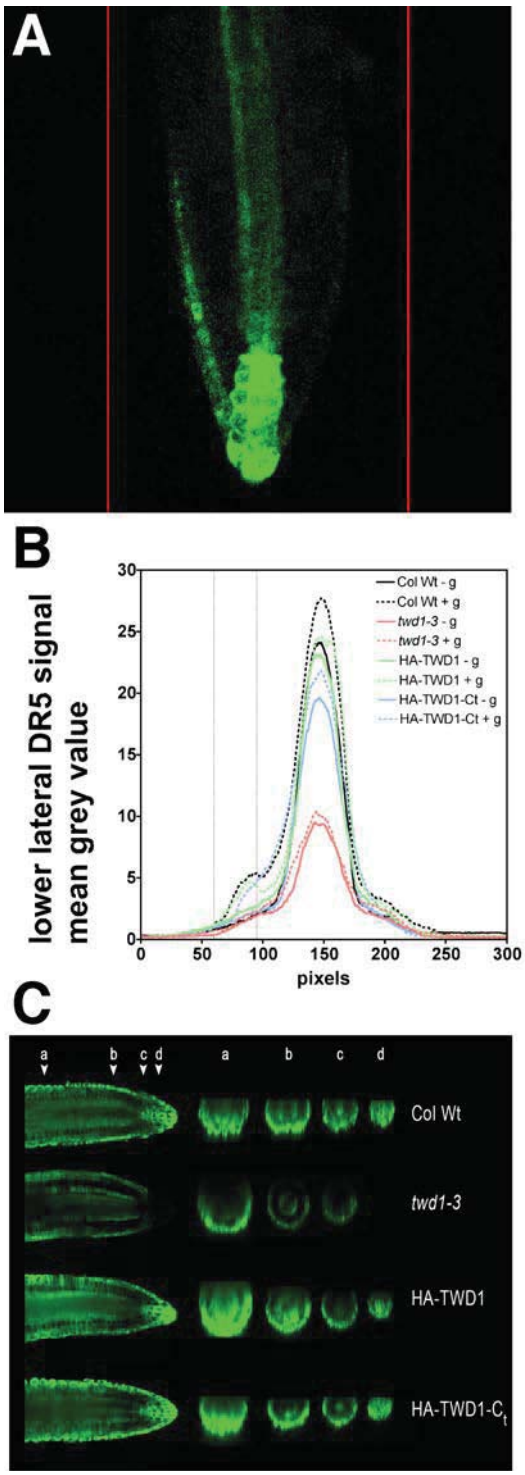

Supplemental Figure 1: Quantification of epidermal DR5:GFP signals at the lower side of wild type (Col Wt), *twd1-3*, HA-TWD1 and HA-TWD1-C_t roots upon gravistimulation.

(A) Confocal image illustrating DR5:GFP signal quantification. Note gravity-induced, basipetal IAA reflux at lower (= left) side of root; red lines mark limits of quantification.

(B) Mean grey values of representative DR5:GFP signals without (**-g**) and with gravistimulation (**+g**).

(C) Sagittal sections (**a - d**) of confocal 3D animations of DR5:GFP images taken from roots incubated for 2h on 100 nM IAA (bottom of roots). Note absence of DR5 induction by IAA in the stele in *twd1-3*.

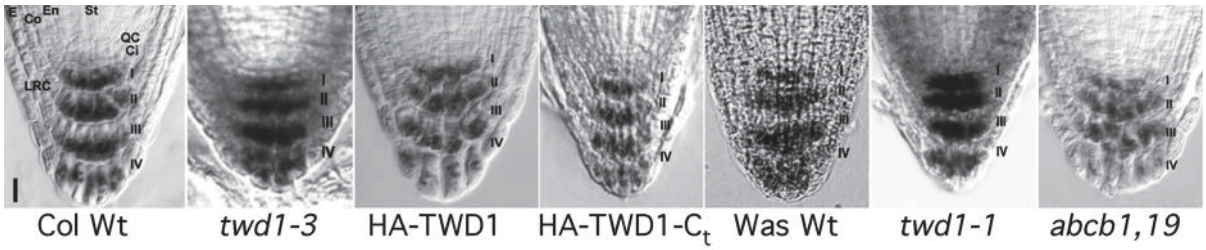

Supplemental Figure 2: Lugol-stain of *Arabidopsis* root tips indicates no signif icant developmental defects in *TWD1*- and *ABCB* loss- and gain-of-function ro ots. Scale bar, 20 µm.

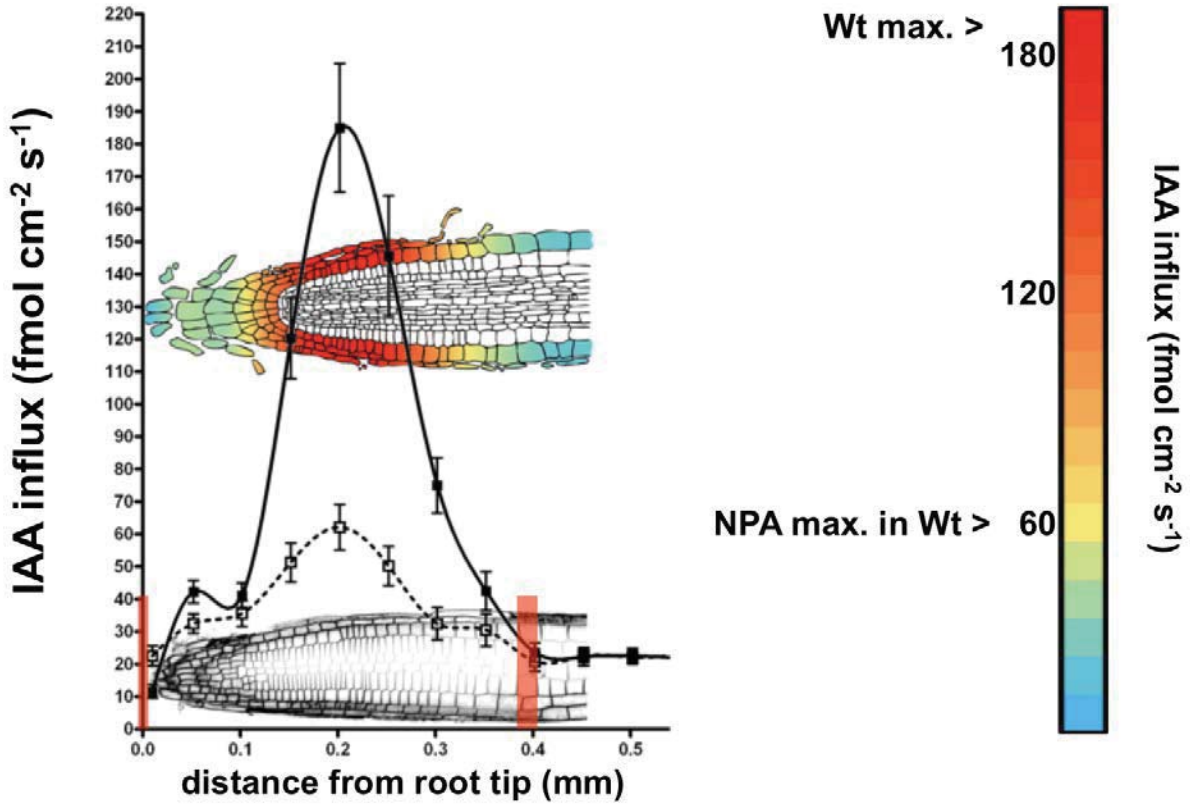

Supplemental Figure 3: Illustration of construction of heat-map presentation of IAA influx profiles along wild-type roots.

Influx profiles were aligned to confocal images of Wt (Col Wt) and *TWD1* loss- and gain of-function alleles/lines using the root tip and begin of DEZ as reference (red bars). Wt influx maxima (180 fmol cm^{-2} s^{-1}) and NPA-induced Wt minima (dashed line; 60 fmol cm^{-2} s^{-1}) at 0.2 mm from the tip were used to calibrate the influx values transferred to a model Arabidopsis root (Swarup et al., 2005). Positive fluxes represent a net IAA influx. Data are means ± S.E. (n = 12).

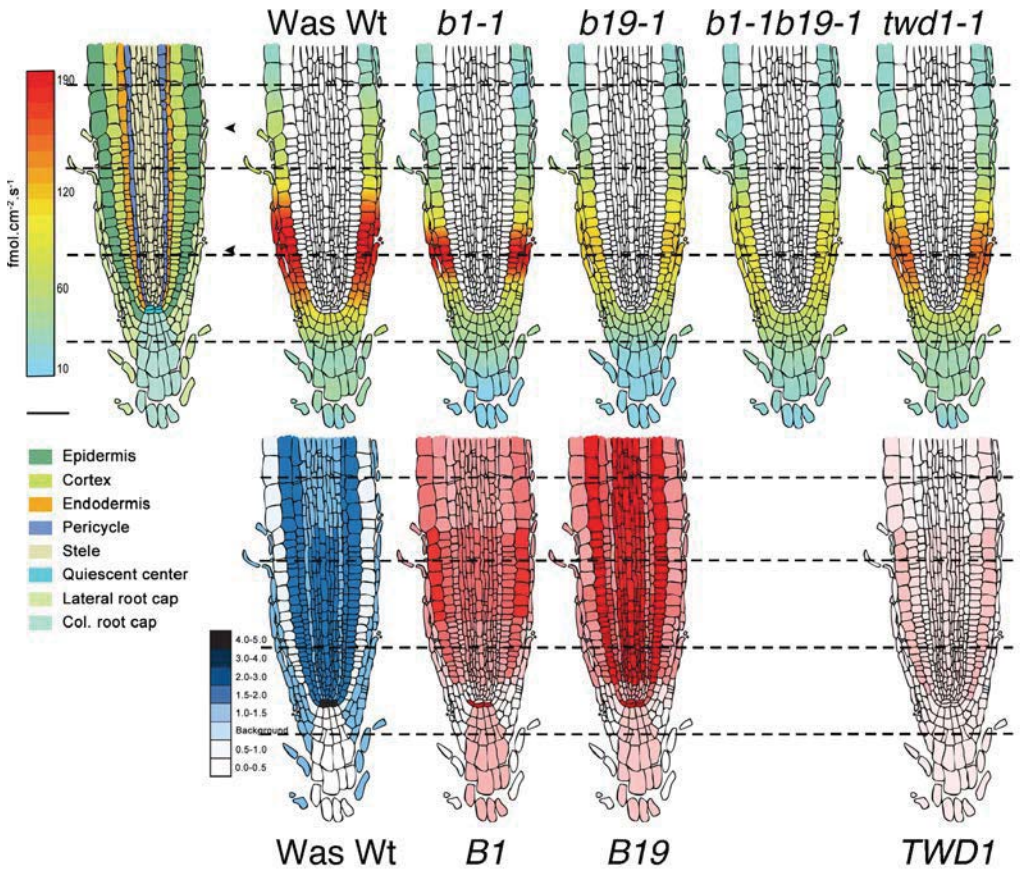

Supplemental Figure 4: Heat-map presentation of IAA influx profiles along wild type (Was Wt), *twd1* and *abcb* roots (all in Was Wt background) measured using an IAA-specific microelectrode. Positive fluxes represent a net IAA influx. Data are means ± S.E. (n = 12). As reference, mapping of root tissues (blue) and high-resolution expression analysis (red; ArexDB: www.arexdb.org) is given. For construction of heat maps, see Supplemental Fig. 3. Bar, 40 µm.

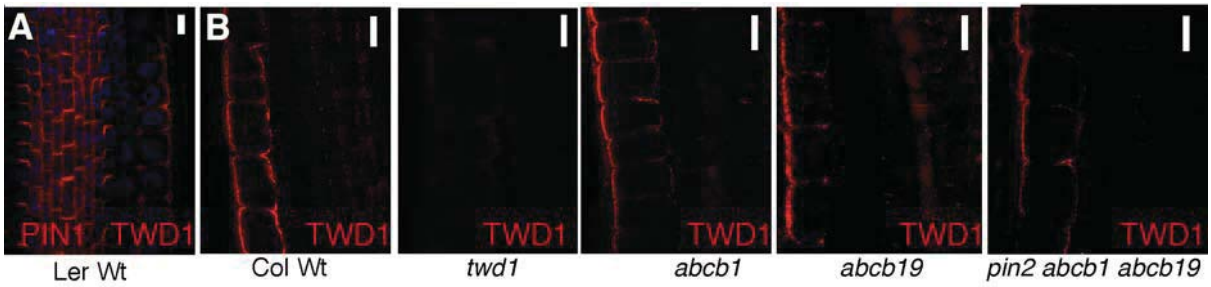

Supplemental Figure 5: TWD1 immunolocalization controls.
(A) Lateral TWD1 signals are not caused by incomplete antisera penetration shown by co-IL of TWD1 (red signals in epidermis) with PIN1 (red signals in stele).
(B) TWD1 immunolocalization (red) is absent in *twd1* (*twd1-3*) and not significantly changed in *abcb* and *pin* mutant backgrounds. Bars, 10 µm.

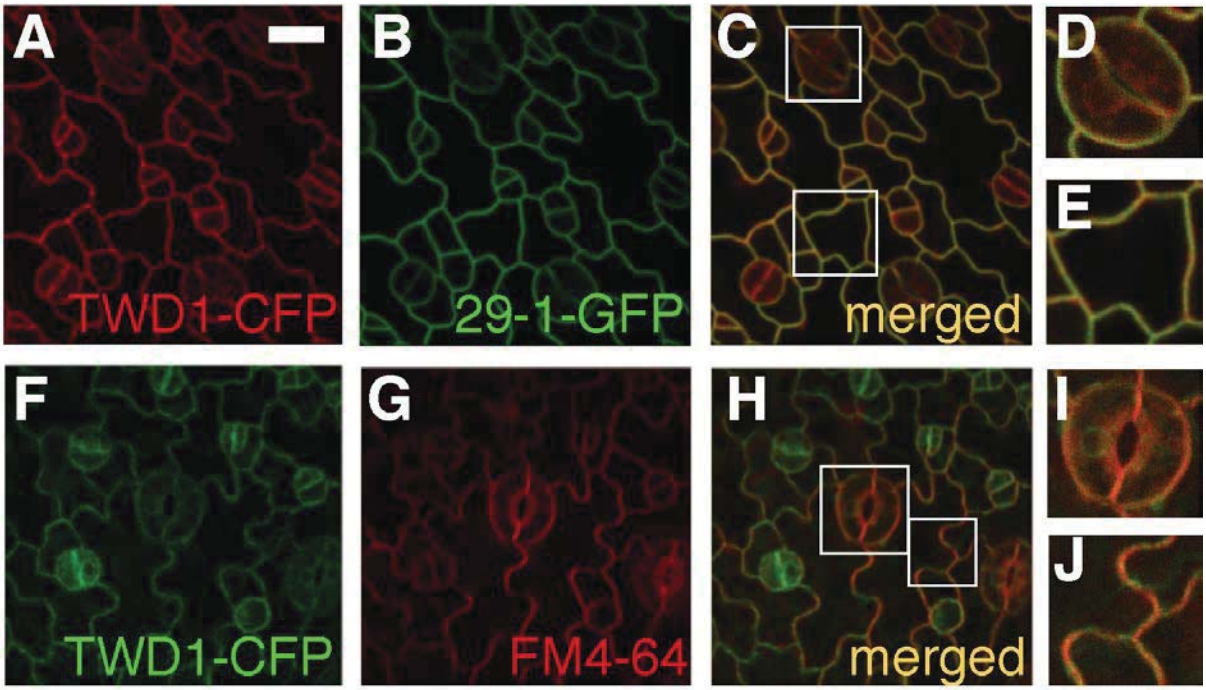

Supplemental Figure 6: TWD1-CFP widely co-localizes with PM markers in the epidermis of first true leaves.
Merged images of TWD1:TWD1-CFP (red or green) with PM markers, 29-1-GFP (**A-E**; green) and FM4-64 (**F-J;** red), indicating co-localization at the plasma membrane (see close-up **D-E** and **I-J** for details). Note that TWD1-CFP signals are less evenly distributed in comparison to those of the PM markers. Further, ER locations for TWD1-CFP are most obvious in stomata (D, I). Bar, 20 μm.

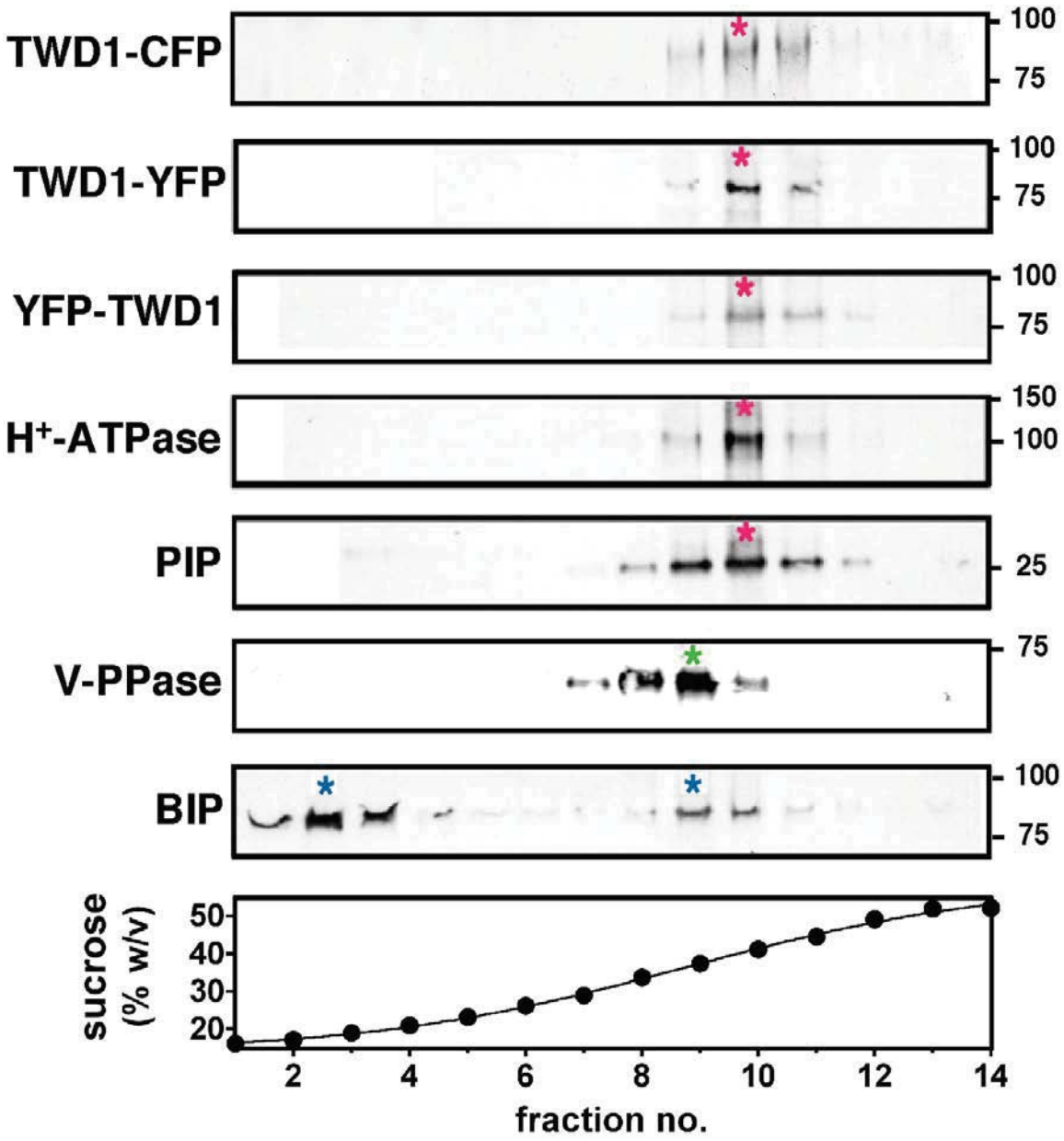

Supplemental Figure 7: Separation of TWD1 microsomes prepared from Arabidopsis plants expressing tagged TWD1 under native or constitutive promoters using discontinuous sucrose gradient centrifugation.
TWD1-CFP (TWD1:TWD1-CFP), TWD1-YFP (35S:TWD1-YFP), YFP-TWD1 (35S:YFP-TWD1) co-migrate with PM markers, H^+-ATPase AHA2 (LIT) and PIP (LIT), in linear sucrose gradients (red asterisks). Note lack of overlap between TWD1 and vacuolar marker, V-PPase (green asterisks) and ER marker, BIP (blue asterisks). Microsome preparation and separation as well as origin of antisera as described elsewhere (Song et al., 2010).

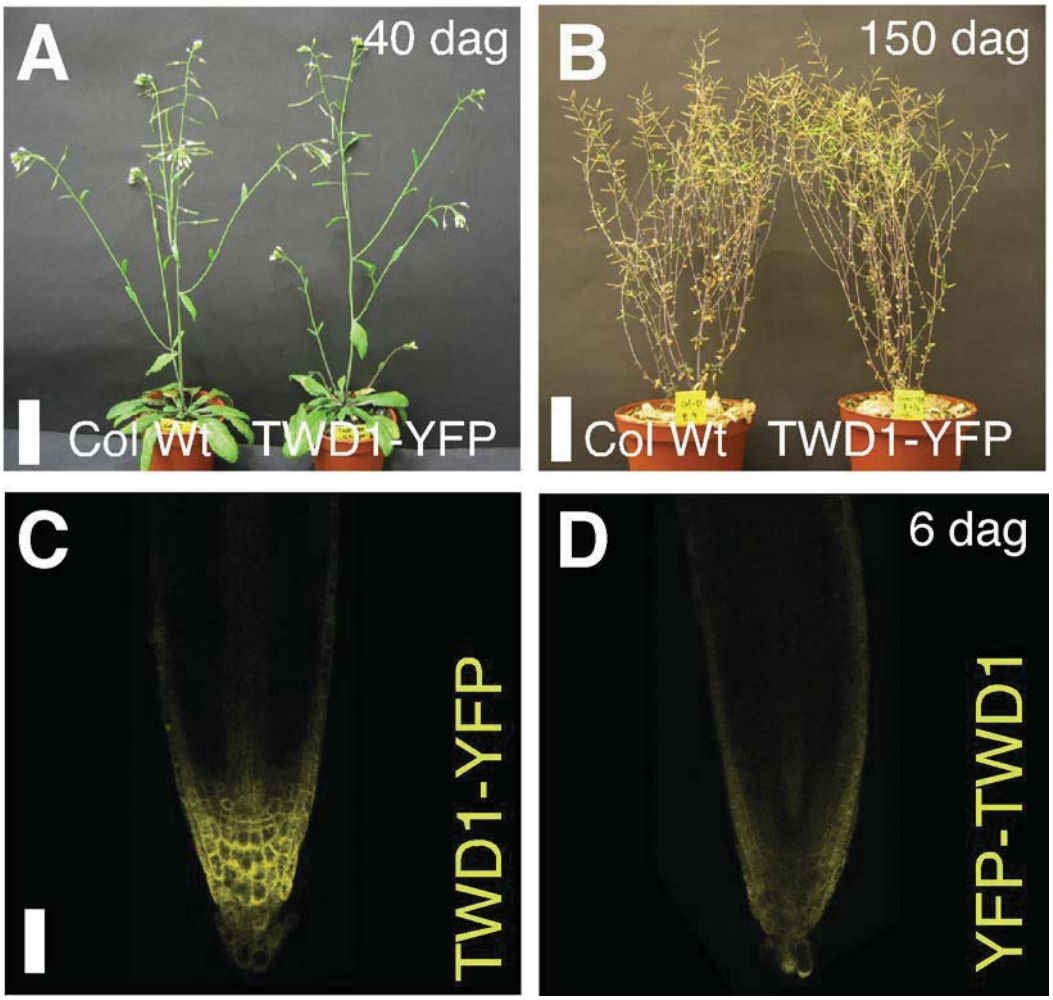

Supplemental Figure 8: TWD1-YFP fusions functionally complement *twd1.*
(A-B) TWD1-YFP complements *twd1-3* to a similar extent under long-day (**A.** 16h light, 40 dag) and short-day (**B.** 8h light, 150 dag) growth conditions. Bars, 5 cm (**A**) and 10 cm (**B**).
(C-D) YFP-TWD1 lines show slightly lower TWD1 expression levels compared to TWD1-YFP correlating with a slightly reduced degree of complementation. Bar, 50 µm.

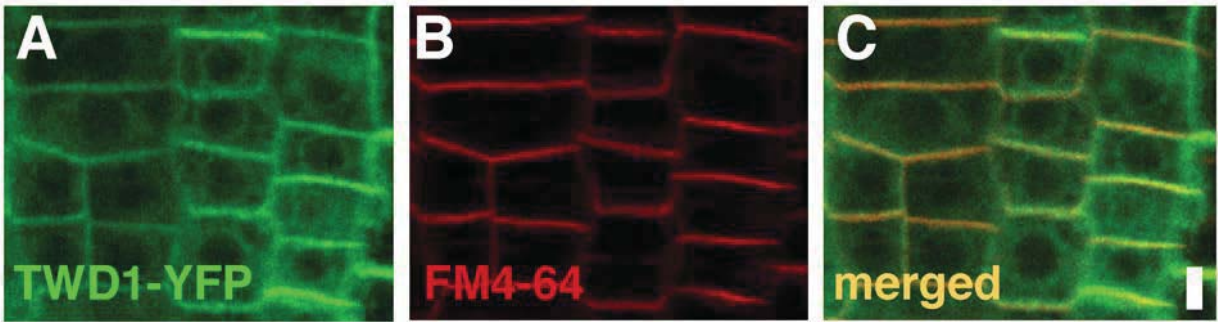

Supplemental Figure 9: TWD1-YFP (**A**) partially co-localizes with PM marker FM4-64 (**B).** Note, yellow PM signals in merged pictures (**C**), indicating PM signals for TWD1-YFP. For close up of merged pictures, see Fig. 6. Bar, 10 μm.

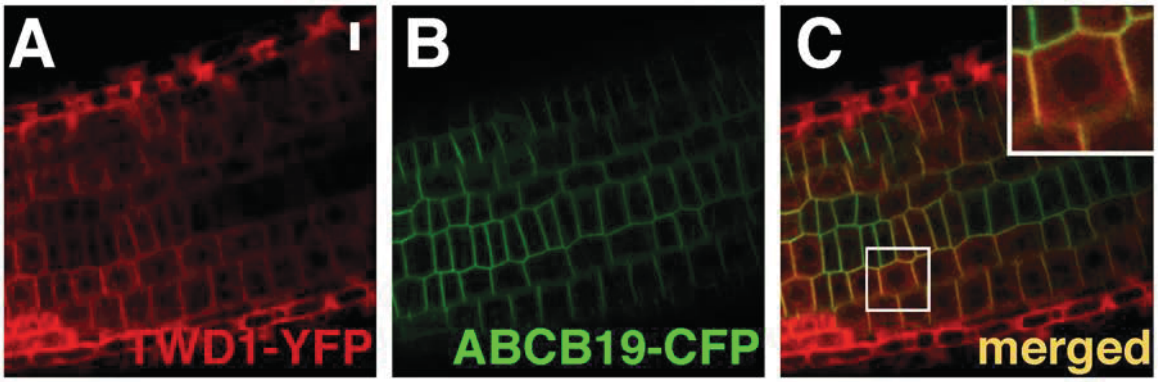

D

	Plasma membrane	*Inner of cell*
r_p (± SD)	0.6141 ± 0.182	0.2473 ± 0.160*
r_s (± SD)	0.5776 ± 0.175	0.2398 ± 0.141**

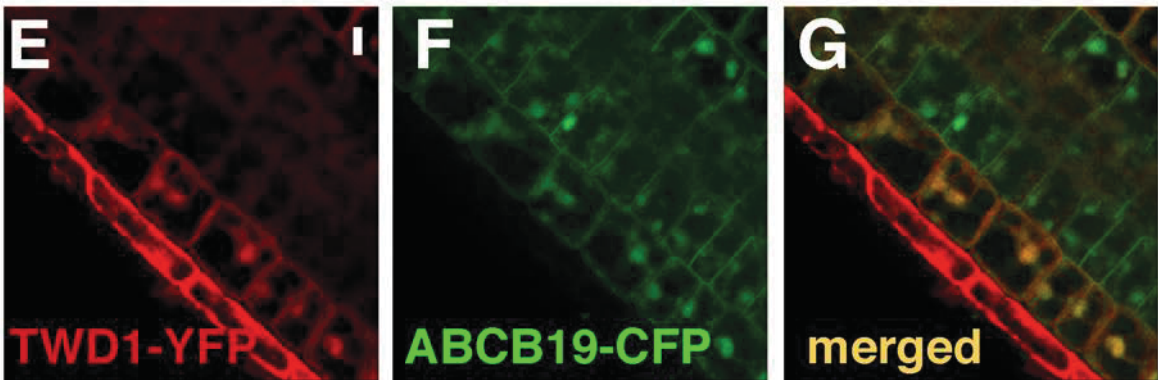

Supplemental Figure 10: TWD1-YFP co-localizes with PM marker, ABCB19-CFP, in the epidermis of roots.

(A-C) Single-channel (**A-B**) and merged images (**C**) of 35S:TWD1-YFP (red) and ABCB19:ABCB19-CFP (green) indicating co-localization at the plasma membrane (see inset for close-up). Note that TWD1-YFP expression and therefore also co-localization is limited to certain planar, epidermal cell files. Bar, 15 µm.

(D) Quantitative correlation of TWD1-YFP and ABCB19-CFP co-localization in the epidermis of *Arabidoposis* roots. Significant signal differences of co-localization in the inner of the cell to plasma membrane values according to one-way ANOVA followed by Dunnet's post-test (r_p, Pearson's correlation coefficient; r_s, Spearman's correlation coefficient) are indicated by one or two asterisks.

(E-G) Co-localization between TWD1-YFP and ABCB19-CFP in BFA-induced (50 µM, 1h) compartments in the meristematic zone. Note that co-localization in BFA compartments is strongest in epidermal cell files. Bar, 10 µm.

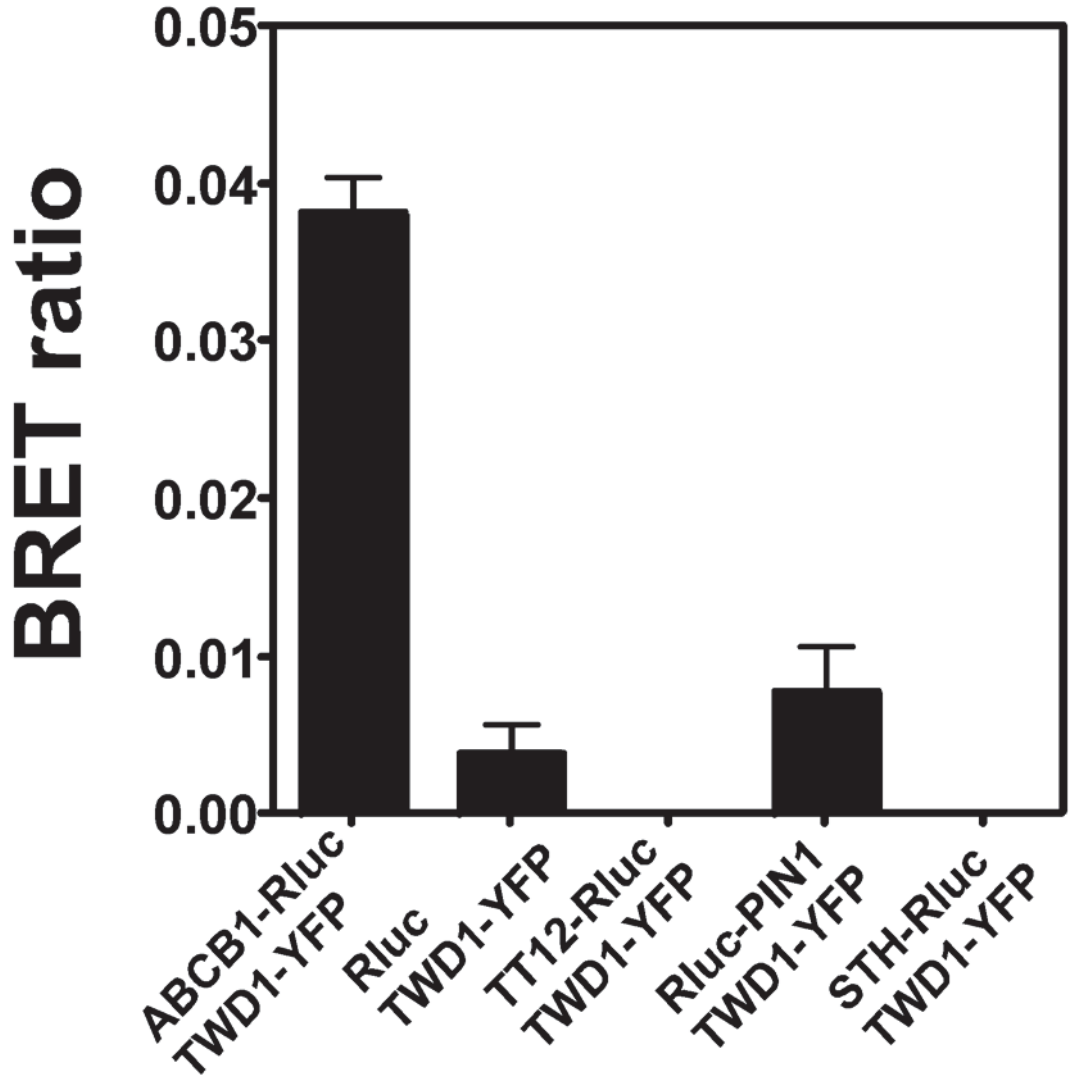

Supplemental Figure 11: Functional interaction between TWD1 and ABCB1.
TWD1-YFP interacts with ABCB1-Rluc assayed by BRET using stable Arabidopsis lines. Note absence of significant BRET signals between TWD1-YFP and unspecific controls, TT12, STH and soluble Rluc alone and low interaction with PIN1. Data are means ± S.E. (n = 4).

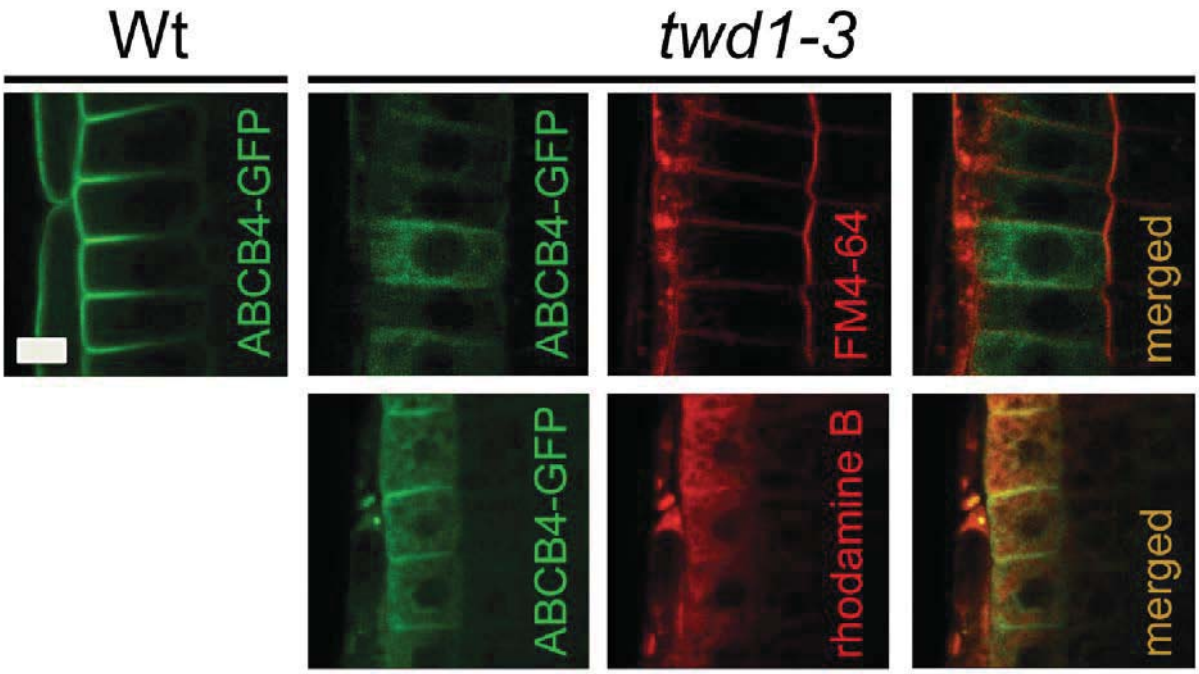

Supplemental Figure 12: ABCB4 is widely delocalized from the PM to the ER in the meristematic zone.
B4 is broadly localized to the ER in *twd1-3* as shown by co-localization with ER marker, hexyl rhodamine B (rhodamine B), but less with PM marker, FM4-64. Bar, 10 µm.

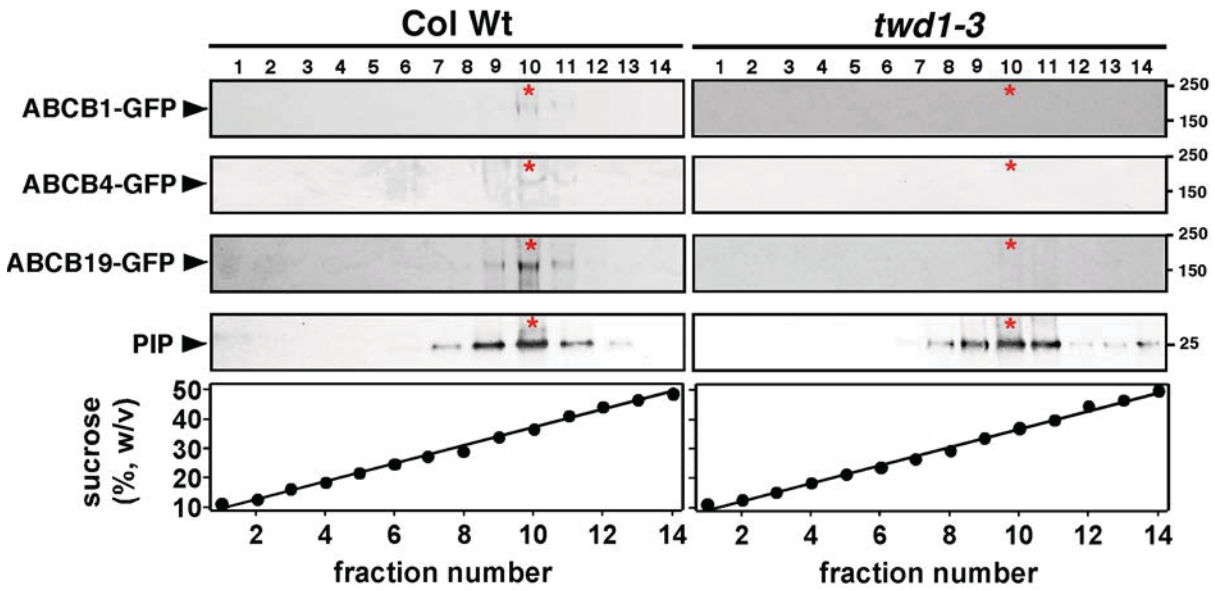

Supplemental Figure 13: ABCB1-, ABCB4- and ABCB19-GFP are degraded in *twd1.*

B1-GFP, B4-GFP and B19-GFP but not the PM marker, PIP, are degraded in *twd1-3* as revealed by Western analysis after linear sucrose gradient centrifugation. Microso me preparation and separation as well as origin of PIP antisera as described elsewh ere (Song et al., 2010).

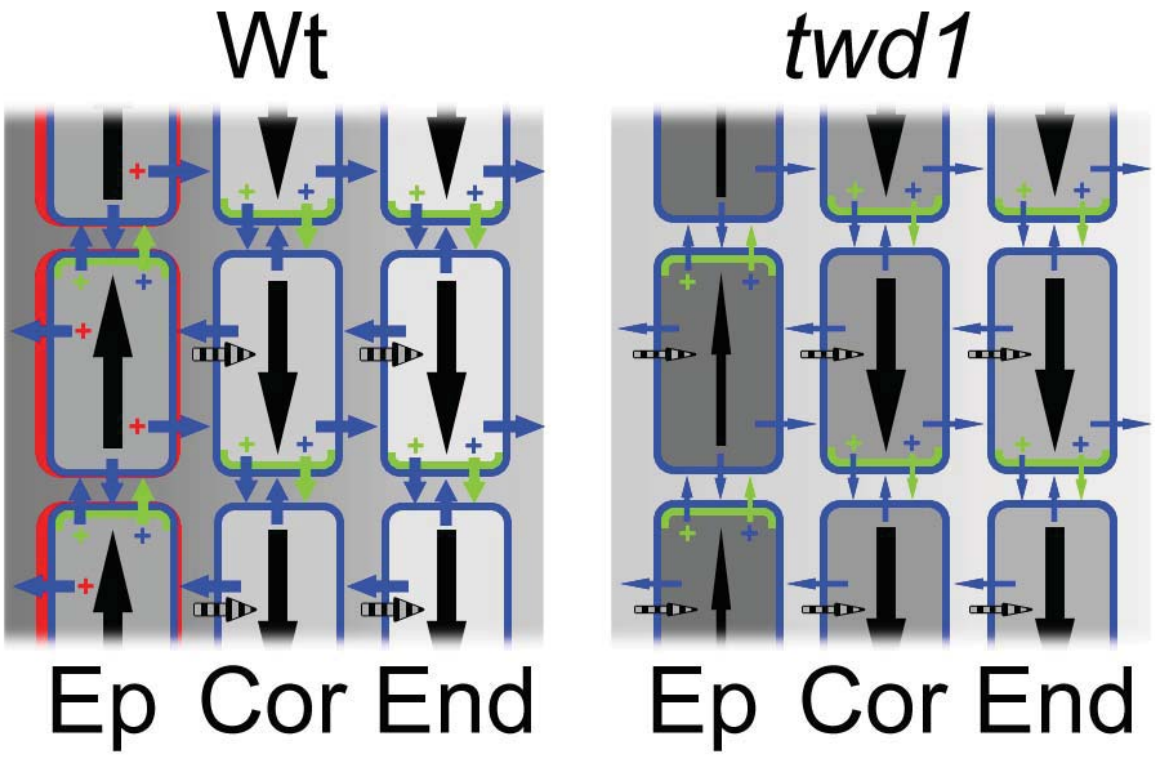

Supplemental Figure 14: Model on the role of TWD1 in promoting lateral ABCB-mediated auxin transport in the root.
In wild-type (**Wt**) roots, the independent and interactive (**+**) action of mostly polarly expressed PINs (**green**) and mostly non-polar expressed ABCBs (**blue**) results in cellular IAA efflux (small colored arrows) providing the basis for vectorial IAA streams (straight black arrows). Laterally, expressed TWD1 (**red**) promotes ABCB-mediated transport (**+**) at lateral sides (mainly outward-facing) of the epidermis minimizing apoplastic reflux (dashed black arrows) and interconversion of epidermal (**Ep**), cortical (**Cor**) and endodermal (**End**) streams. In ***twd1*** roots, epidermal ABCB action is widely lost allowing apoplastic reflux, which is reducing basipetal (shoot-ward) PAT enhancing total IAA level.

Supplemental References

Song, W.Y., Choi, K.S., Kim do, Y., Geisler, M., Park, J., Vincenzetti, V., Schellenberg, M., Kim, S.H., Lim, Y.P., Noh, E.W., Lee, Y., and Martinoia, E. (2010). Arabidopsis PCR2 is a zinc exporter involved in both zinc extrusion and long-distance zinc transport. Plant Cell **22**: 2237-2252.

Swarup, R., Kramer, E.M., Perry, P., Knox, K., Leyser, H.M., Haseloff, J., Beemster, G.T., Bhalerao, R., and Bennett, M.J. (2005). Root gravitropism requires lateral root cap and epidermal cells for transport and response to a mobile auxin signal. Nature Cell Biology **7**: 1057-1065.